Inorganic Chemistry

Article

pubs.acs.org/IC

Ab Initio Chemical Synthesis of Designer Metal Phosphate Frameworks at Ambient Conditions

Alok Ch. Kalita,[†] Nayanmoni Gogoi,[‡] Ritambhara Jangir,[†] Subramaniam Kuppuswamy,[†] Mrinalini G. Walawalkar,[†] and Ramaswamy Murugavel*,[†]

[†]Department of Chemistry, Indian Institute of Technology-Bombay, Powai, Mumbai 400076, India

[‡]Department of Chemical Sciences, Tezpur University, Napaam 784028, India

Supporting Information

ABSTRACT: Stepwise hierarchical and rational synthesis of porous zinc phosphate frameworks by predictable and directed assembly of easily isolable tetrameric zinc phosphate $[Zn(dipp)(solv)]_4$ ($dippH_2$ = diisopropylphenyldihydrogen phosphate; solv = CH_3OH or dimethyl sulfoxide) with D4R (double-4-ring) topology has been achieved. The preformed and highly robust D4R secondary building unit can be coordinatively interconnected through a varied choice of bipyridine-based ditopic spacers L1−L7 to isolate eight functional zinc phosphate frameworks, $[Zn_4(dipp)_4(L1)_{1.5}(DMSO)]\cdot 4H_2O$ (**2**), $[Zn_4(dipp)_4(L2)_{1.5}(CH_3OH)]$ (**3**), $[Zn_4(dipp)_4(L1)_2]$ (**4**), $[Zn_4(dipp)_4(L3)_2]$ (**5**), $[Zn_4(dipp)_4(L4)_2]$ (**6**), $[Zn_4(dipp)_4(L5)_2]$ (**7**), $[Zn_4(dipp)_4(L6)_2]$ (**8**), and $[Zn_4(dipp)_4(L7)_2]$ (**9**), in good yield. The preparative procedures are simple and do not require high pressure or temperature. Surface area measurements of these framework solids show that the guest accessibility of the frameworks can be tuned by suitable modification of bipyridine spacers.

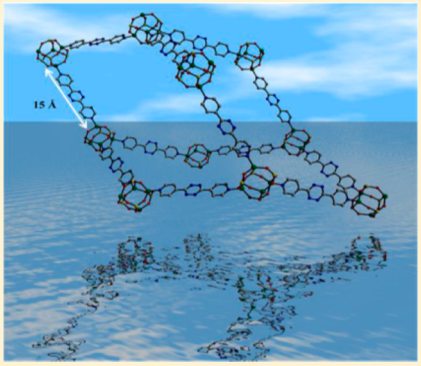

INTRODUCTION

The discovery of microporous aluminophosphates $(AlPO)_x$ by Flanigen and co-workers in 1982 resulted in an outburst of activity in the area of porous solids due to their potential utility in a wide range of applications.[1] Consequently, a host of open framework microporous metal phosphates have been reported, and many of these materials have found applications in sorption, catalysis, magnetism, etc.[2−6] In this context, a rational or retrosynthetic approach for assembling designer phosphate or silicate porous materials from preformed molecular building blocks is of paramount importance. Control over the volume and architecture of the pores or the ability to modify their chemical/physical environments has remained a major unsolved challenge for several decades. Several research groups have focused their investigations toward this objective, since such zeolite modifications will eventually allow the modulation of framework−guest interactions and thus lead to tailored properties and functions. However, the process of assembling designer silicate- or phosphate-based materials has turned out to be a formidable challenge, due to the nonavailability of soluble precursors bearing SiO_4 or PO_4 tetrahedra. It was believed in 1990s that the isolation of compounds such as the kinetically stabilized organosilanetriols, $(R'RN)Si(OH)_3$ (R = aryl; R′ = $SiMe_3$), would eventually afford an easy access to porous solids via $Si_4O_{12}M_4$ molecular cages that resemble the secondary building units (SBUs) found in zeolites.[7−9] Starting from organic-soluble phosphonic acids and phosphate esters, a similar but not identical approach was also envisaged to assemble porous solids.[10,11] No doubt both of these approaches, involving silanols and phosphonic acids, yielded a plethora of structurally diverse secondary building blocks,[7−9] however, it has not been possible to convert any of these M-siloxane or -phosphonate SBUs into porous solids by appropriate chemical modifications or reactions.

A few years ago, we had shown that the reaction of $Zn(OAc)_2\cdot 2H_2O$ with diisopropylphenyl dihydrogen phosphate ($dippH_2$) in methanol produces a zinc phosphate, $[Zn(dipp)(CH_3OH)]_n$.[11a−c] The inability to obtain good-quality single crystals for this species, owing to the rapid loss of methanol, prevented the exact determination of the form of association (cluster versus layered solid). This led us to replace methanol by a stronger Lewis base; for example, substituted pyridines establish that the association number in these system in fact is four.[11] The core of these tetrameric clusters adopts a cubane-like shape that resembles the double-4-ring (D4R) SBUs of zeolitic materials (Figure 1). The fact that there are four zinc centers occupying the alternate corners of the cubane (as if at the four vertices of a tetrahedron) and that they are highly Lewis acidic led us to anticipate the possibility of interconnecting the cubanes by employing bridging ligands with stronger Lewis basic character. However, all attempts to link the D4R cages by bridging Zn centers through bidentate Lewis bases such as 4,4′-bipyridine or its extended analogues persistently yielded an insoluble noncrystalline precipitate. This precluded precise structural analysis of the resulting products by

Received: April 6, 2014
Published: August 14, 2014

   dx.doi.org/10.1021/ic500810d | *Inorg. Chem.* 2014, 53, 8959−8969

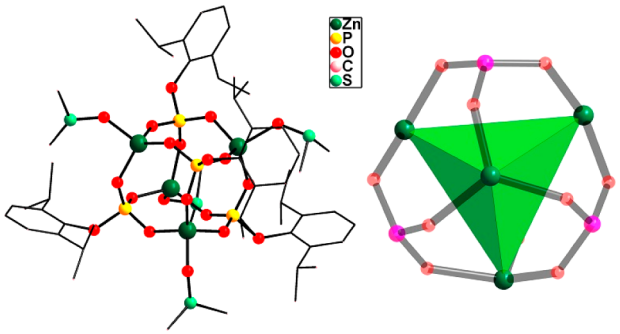

Figure 1. Left: Molecular structure of **1**, right: diagram showing the tetrahedral Zn_4 unit in **1**.

diffraction studies. The process of interlinking D4R cubanes by using ditopic N-donor ligands is exceedingly facile, and therefore the resulting polymeric frameworks rapidly precipitate out of the reaction mixture. Similar difficulties have also been experienced while attempting to covalently link metal phosphonate D4R cages into coordination frameworks.[12] It is pertinent to note here that the use of pyridine-based ancillary ligands and a judicious choice of additional functionality present on the pyridine ring eventually has allowed the noncovalent linking of the D4R cages into hierarchical supramolecular assemblies.[11] Meanwhile it was anticipated that controlled bridging D4R zinc phosphate cubanes can be possibly achieved by employing a preformed zinc phosphate cubane and ditopic spacers shown in Chart 1. Results obtained during this course of study have been reported in this contribution.

Chart 1. Ditopic N-Donor Spacers Used in the Present Study

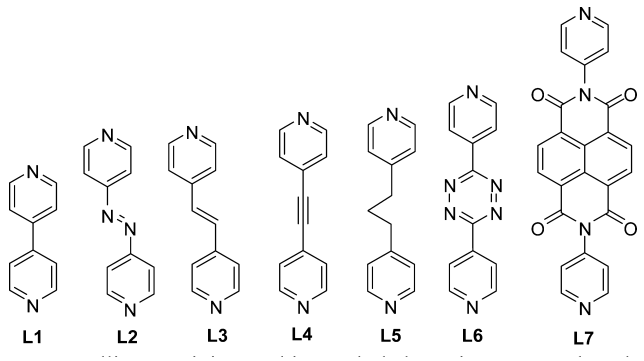

RESULTS AND DISCUSSION

Synthesis and Characterization of [Zn(dipp)(DMSO)]$_4$ (1). Reaction of $Zn(OAc)_2{\cdot}2H_2O$ and $dippH_2$ in a methanol and DMSO mixture yields $[Zn(dipp)(DMSO)]_4$ (**1**) (Scheme 1) as colorless block-type crystals in 85% yield. Analytical and spectroscopic analysis of this product conform satisfactorily well with the tetrameric formulation. The FT-IR spectrum of **1** features strong absorption bands at 1175, 1019, and 918 cm^{-1} due to P═O stretching vibrations and M−O−P asymmetric and symmetric stretching vibrations, respectively (Table S1).[11] The ^{1}H NMR spectrum of **1** shows well-separated peaks for all protons of dipp (2,6-di-isopropylphenylphosphate) (Figure S1). One multiplet at δ 6.9−7.0 ppm is due to the aromatic protons of the dipp ligand. A septet resonance at δ 3.8 ppm is due to the −CH protons of the isopropyl group of dipp. A

Scheme 1. Synthesis of Zinc Phosphate Frameworks 2−9 Using Ditopic N-Donor Spacers L1−L7

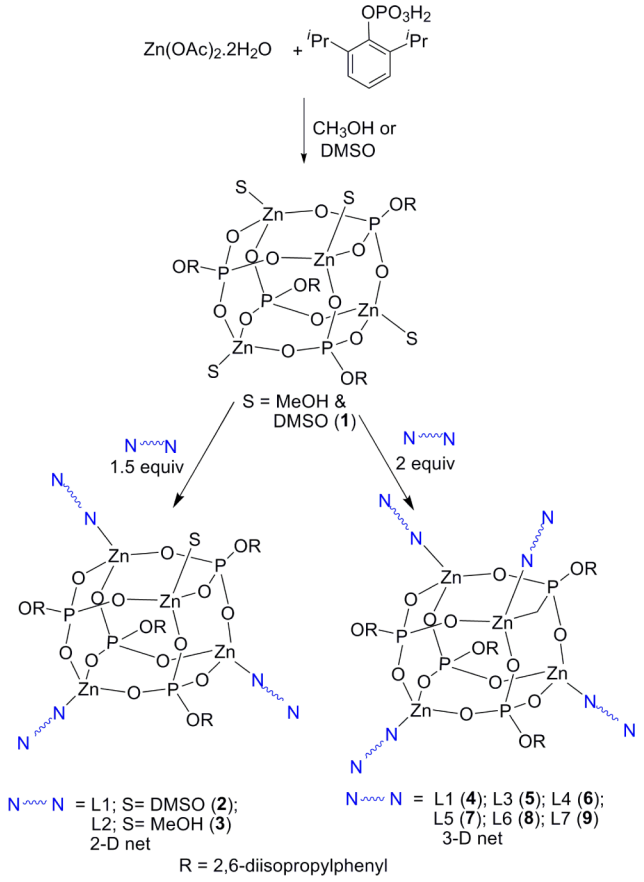

doublet appears at 1.1 ppm due to the $-CH_3$ protons of the isopropyl group of the dipp ligand. Again the ^{31}P NMR spectrum shows a nearly identical chemical environment for the phosphorus atoms and shows a resonance at δ −5.2 ppm.

Block-shaped colorless single crystals of **1** crystallize in triclinic space group $P\bar{1}$. A perspective view of the molecular structure is shown in Figure 1. The structure and bond parameters of **1** are similar to zinc phosphate cubanes described earlier in the literature.[11] The observed average P−O distance inside the cage is 1.533 Å, while the average Zn−O distance is 1.931 Å. The average Zn−O−P angle is 134.8°, which is considerably smaller than the 180° that would be expected for a linear edge. The zinc and phosphorus atoms remain largely tetrahedral. The dimensions of the cubic core can best be understood from the distances of Zn···P edges (av 3.157 Å), P···P face diagonals (av 4.618 Å), Zn···Zn face diagonals (av 4.299 Å), and Zn···P body diagonals (av 5.460 Å). In addition, D4R cages are connected through C−H···O intermolecular hydrogen-bonding interactions (H43···O31, 2.515 Å) (Figure 2).

Meanwhile it was envisaged that a stepwise hierarchical assembling route might be successful in coordinatively connecting the D4R cages. It can be easily visualized that by linking two D4R cages through one bridging ligand, it might be possible to isolate a dimeric species. Linking two Zn centers on each D4R cage may result in either a 1D assembly or a cyclic tetrameric species. Similarly if three or four Zn centers per D4R cage are interconnected, then two- or three-dimensional frameworks will result, respectively. In order to control the

dx.doi.org/10.1021/ic500810d | Inorg. Chem. 2014, 53, 8959−8969

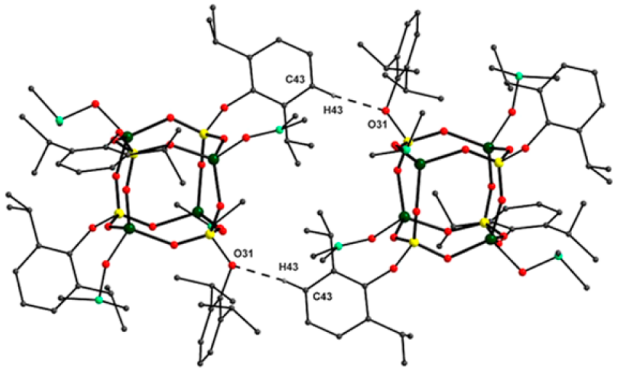

Figure 2. 22-Membered macrocycle formation through C−H···O hydrogen-bonding interactions in **1**.

degree of association, it was anticipated that [Zn(dipp)-(DMSO)]$_4$ will possibly serve as a superior precursor due to the slightly more Lewis basic nature of DMSO as compared to CH_3OH.

Synthesis and Characterization of [Zn$_4$(dipp)$_4$(L1)$_{1.5}$-(DMSO)]·4H$_2$O (2). The reaction of Zn(OAc)$_2$·2H$_2$O, dipp-H$_2$, and 4,4′-bipyridine (L1) in a CH_3OH−DMSO mixture yielded single crystals of [Zn$_4$(dipp)$_4$(L1)$_{1.5}$(DMSO)]·4H$_2$O (**2**) (Scheme 1). X-ray diffraction studies unambiguously establish that **2** is a robust 2D coordination framework that crystallizes in the monoclinic *Pc* space group and is built by interlinking three Zn centers per D4R cage with bipyridine bridges.

The coordination environment of zinc and phosphorus centers are the same as that of **1**. Three of the total four Zn ions are four coordinated, with three phosphate O atoms from three different dipp ligands and one N atom from the 4,4′-bipy ligand (Zn−O 1.906(9)−1.932(8) Å; Zn−N 2.037(1)−2.062(1) Å) to show tetrahedral geometry (Figure 3). The average P−O

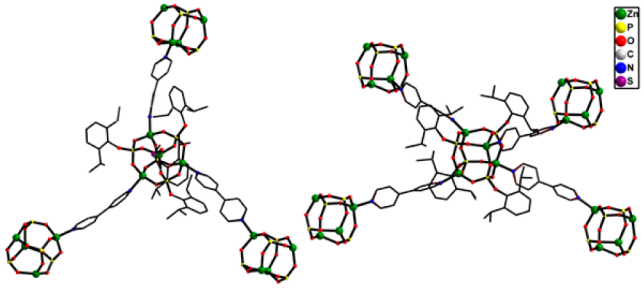

Figure 3. View of the three-connected and four-connected nodes linked by spacer L1 in **2** and **4**.

bond length (1.555 Å) is significantly shorter than that of a P−O single bond (∼1.60 Å) but is considerably longer than that of a P═O double bond (∼1.45−1.46 Å). Interestingly the fourth Zn center of the D4R cage remains occupied by a DMSO ligand and therefore does not participate in the interlinking process and helps in the formation of the 2D layer. The fourth Zn center is coordinated with three phosphate O atoms from three different dipp ligands and one oxygen atom from a DMSO molecule (Zn−O 1.925(9)−1.991(1) Å). Thus, the D4R cages can be regarded as pyramidal three-connected nodes due to the presence of coordinated DMSO at one of the edges occupied by the Zn center, and this eventually leads to the formation of a 2D framework structure with a cyclohexane-like basic repeating unit (Figure 4). Compound **2** represents a hitherto unknown 2D framework made up of 6,3-sheets,

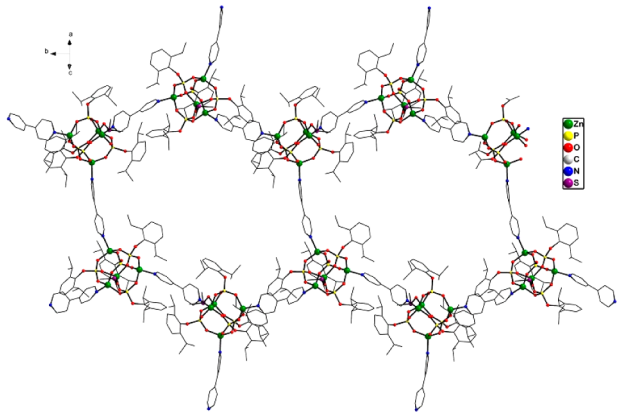

Figure 4. 2D polymeric network structure of **2**.

wherein a zeolitic SBU has been rationally interconnected through coordinate linkages. Figure 3 also depicts how a four-connected 3D network, compound **4**, can be produced from the same set of starting materials through a careful control of stoichiometry and dilution (details below).

Synthesis and Characterization of [Zn$_4$(dipp)$_4$(L2)$_{1.5}$-(CH$_3$OH)] (3). Intriguingly, an isoreticular 2D framework, [Zn$_4$(dipp)$_4$(L2)$_{1.5}$(CH$_3$OH)] (**3**), has also been subsequently isolated from the reaction of Zn(OAc)$_2$·2H$_2$O and dipp-H$_2$ with 1,2-di(pyridin-4-yl)diazene (L2) in methanol. In this case, slow diffusion of reactants due to high dilution assisted the isolation of the single-crystalline product. The FT-IR spectrum of **3** features characteristic P═O stretching and M−O−P asymmetric and symmetric stretching vibrations at 1175, 1020, and 916 cm^{-1}, respectively (Table S1).[11] The ^{1}H NMR spectrum of **3** in DMSO-d_6 shows well-separated peaks for protons of dipp and L2 (Figure S3). One multiplet at δ 6.98 ppm is due to the aromatic protons of four dipp ligands. Doublet resonances at δ 7.80, 8.25, and 8.84 ppm can be attributed to the protons of the L2 ligand. The expected septet resonance due to the −CH protons of the isopropyl group of dipp around δ 3.6 ppm is masked by the broad signal of H_2O centered at 3.33 ppm. CH_3 protons of coordinated methanol are observed as a singlet at 3.19 ppm, and the doublet centered at 1.08 ppm can be easily attributed to the $-CH_3$ protons of the isopropyl group of the dipp ligand. Integration of the ^{1}H NMR spectrum suggests formation of a supramolecular assembly with a dipp:L2 ratio of 4:1.5.

Bright red rectangular crystals suitable for X-ray diffraction were obtained from a methanol solution at room temperature. Single-crystal X-ray analysis revealed that compound **3** crystallizes in the monoclinic space group $P2_1/c$ and is polymeric in nature. A perspective view of the D4R zinc phosphate repeating unit structure in compound **3** is shown in Figure 5, while pertinent bond lengths and angles are listed below. The crystal structure of **3** is constructed from a D4R zinc phosphate, [Zn$_4$(dipp)$_4$(abpy)$_{1.5}$(CH$_3$OH)], bridged together by azobipyridine to form a two-dimensional coordination polymer (Figure 6) through a cyclohexane-like repeating unit (Figure 7). The repeating unit is built of a cubic framework, and zinc and phosphorus atoms occupy the alternate vertices. The Zn···P edges of the cubane are bridged by a phosphate oxygen in a μ_2 fashion, resulting in the

dx.doi.org/10.1021/ic500810d | Inorg. Chem. 2014, 53, 8959−8969

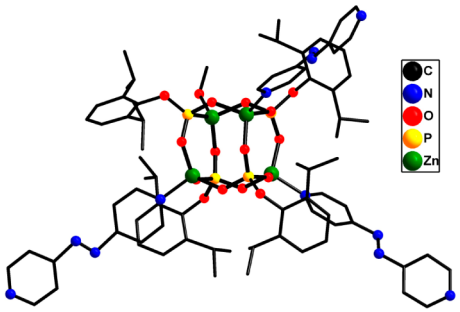

Figure 5. Ball-and-stick model of the D4R core bridged by L2 in **3**. Hydrogen atoms have been omitted for clarity.

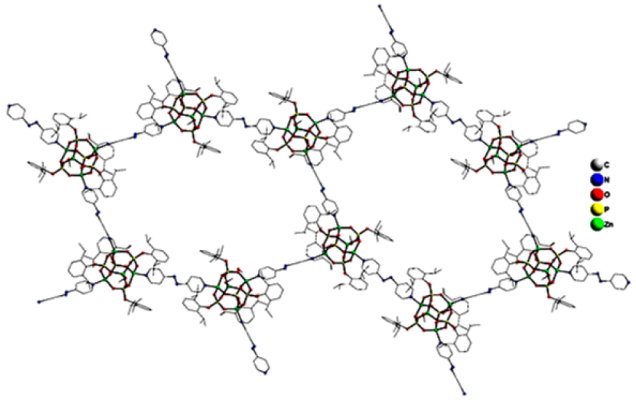

Figure 6. 2D polymeric network of **3**.

formation of six nonplanar $Zn_2O_4P_2$ eight-membered rings with distorted pseudo-C_4 crown conformation. The bond parameters found in **3** are comparable to earlier reported zinc phosphates and phosphonates in the literature.[11,13] The average P−O distance (1.532 Å) is significantly shorter than that of a P−O single bond (∼1.60 Å), but is considerably longer than that of a P═O double bond (1.45−1.46 Å).[11] The average Zn−O distances in **3** vary slightly from each other (1.916 Å). The average Zn−O−P angles along the cubane edges (139.9°) are smaller than the 180° that would be expected for a linear edge, thus providing a spherical shape for the cubane structure. The zinc and phosphorus atoms in all the complexes remain essentially tetrahedral. The dimensions of the cubic core in **3** can best be understood from the distances of Zn···P edges (3.160(1) Å), P···P face diagonals (4.620(3) Å), Zn···Zn face diagonals (4.307(3) Å), and Zn···P body diagonals (5.475(3) Å). There are two distinct types of zinc centers in **3** based upon their coordination environments. While the fourth coordination sites of Zn1, Zn2, and Zn3 are fulfilled by exocyclic azobipyridines, in the case of Zn4 the fourth coordination site is occupied by a coordinated methanol. The three azobipyridines coordinated to Zn1, Zn2, and Zn3 coordinate to the zinc centers in the nearby Zn_4P_4 entity, thus covalently bridging the D4R cubanes. However, due to the presence of coordinated methanol, such a covalent linking between the D4R cubanes was possible only from three edges, thus leading to the formation of a 2D coordination polymer as shown in Figure 6. The space-filling model depicted in Figure S4 shows the presence of voids within the 2D framework.

Analysis of the 2D framework in **3** by Topos reveals that the D4R cages act as pyramidal three-connected nodes and form 6,3-sheets (or 2D networks) stacked on top of each other (Figure S4).[14] Even though both **2** and **3** are 2D frameworks, their isolation emphasizes the feasibility of these approaches to assemble porous zinc phosphate frameworks by adequate optimization of the reaction conditions. Since the addition of DMSO to the reaction mixture allowed us to control the degree of association and isolate **2**, it was envisaged that reacting the easily isolable complex $[Zn(dipp)(DMSO)]_4$ with bipyridine spacers is possibly a superior route to interconnect the D4R cages at all four edges.

Synthesis and Characterization of $[Zn_4(dipp)_4(L1)_2]$ (4). Reaction of $[Zn(dipp)(DMSO)]_4$ with L1 in methanol medium yielded $[Zn_4(dipp)_4(L1)_2]$ (**4**) as a single-crystalline product. Analytical and spectroscopic analyses of the product conform satisfactorily well with expected values (Table S1). The FT-IR spectrum of **4** features characteristic P═O stretching vibrations and M−O−P asymmetric and symmetric stretching vibrations at 1175, 1020, and 916 cm^{-1}, respectively (Figure S5).[11] The ^1H NMR spectrum of **4** shows well-separated peaks for all protons of dipp and bipyridine moieties (Figure S5). Two doublet resonances at δ 8.7 and 7.8 ppm are due to the protons of the bipyridyl ligand. One multiplet at δ 6.9 ppm is due to the aromatic protons of the dipp ligand. A

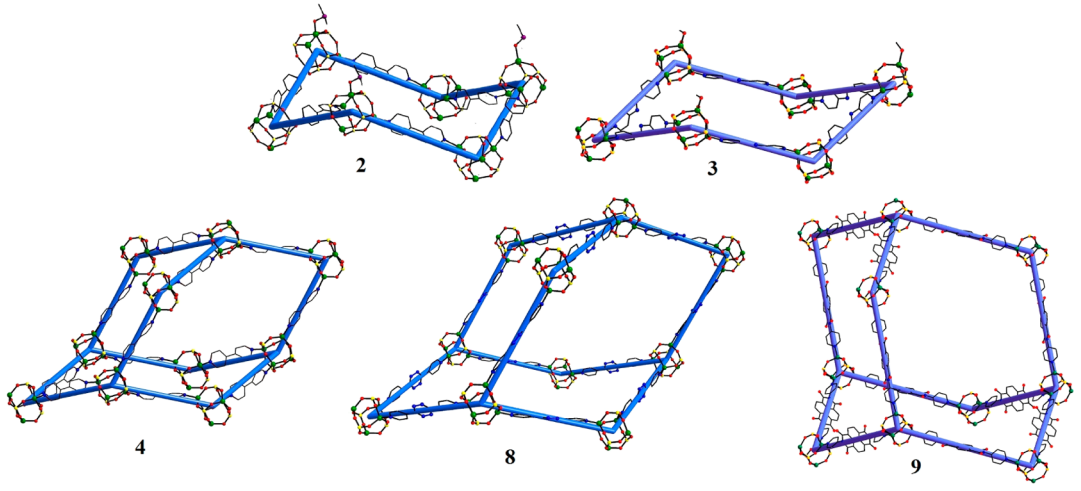

Figure 7. Top: Cyclohexane-like unit formation in two-dimensional phosphates **2** and **3**. Bottom: Adamantane-like repeating unit formation in three-dimensional phosphates **4**, **8**, and **9** (intercubane distances in **4**, **8**, and **9** are 11.021(6), 15.075(1), and 19.353(1) Å, respectively).

dx.doi.org/10.1021/ic500810d | Inorg. Chem. 2014, 53, 8959−8969

septet resonance at δ 3.6 ppm is due to the −CH protons of the isopropyl group of dipp. A doublet appears at 1.1 ppm due to the $-CH_3$ protons of the isopropyl group of the dipp ligand. Integration of the ^{1}H NMR spectrum gives an idea of formation of supramolecular assemblies where the dipp:bipyridine ratio is 1:0.5. Again the ^{31}P NMR spectrum shows a nearly identical chemical environment for the phosphorus atoms and shows a resonance at δ −5.2 ppm. It is well known in the literature that zinc phosphates and phosphonates have been known to show interesting optical properties especially in the presence of bipyridine and phenanthroline coligands.[15] Hence the optical properties for compound **4** have been carried out in solution. Absorption observed at 265 nm for **4** is typical charge-transfer absorption.

Compound **4** crystallizes in the orthorhombic *Fdd*2 space group. Individual D4R zinc phosphate cages in **4** act as tetrahedral four-connected nodes bridged together by 4,4′-bipyridine spacers (Figures 3 and 7). Compound **4** is built on a cubic framework where zinc and phosphorus atoms occupy alternate vertices. Each of the Zn···P edges of the cubane is bridged by a phosphate oxygen atom in a μ_2 fashion, which results in the formation of six nonplanar $Zn_2O_4P_2$ eight-membered rings; it therefore adopts a distorted pseudo-C_4 crown conformation.

The bond parameters found in these complexes are comparable to zinc phosphates and phosphonates published in the literature.[11,13] As shown in Figure 3, the asymmetric unit of **4** contains four similar Zn centers. The Zn ion is four coordinated, with three phosphate O atoms from three different dipp ligands and one N atom from the 4,4′-bipy ligand (Zn−O 1.865(3)−1.950(2) Å; Zn−N 1.994(3)−2.043(3) Å) to show tetrahedral geometry (Figure S6). The average P−O bond length (1.536 Å) is significantly shorter than that of a P−O single bond (∼1.60 Å) but is considerably longer than that of a P═O double bond (∼1.45−1.46 Å).

The average Zn−O−P angles along the cubane edges (135.06°) are smaller than the 180° that would be expected for a linear edge, thus providing a spherical shape to the cubane structure. The dimensions of the cubic core in **4** can best be understood from the distances of the Zn···P edges (3.09(1)−3.28(1) Å), P···P face diagonals (4.5678(3)−4.765(7) Å), Zn···Zn face diagonals (4.301(1)−4.25(6) Å), and Zn···P body diagonals (5.428(1)−5.484(5) Å). Each D4R zinc phosphate is connected through N atoms of 4,4′-bipy ligands to Zn(II) centers of another D4R, which continues in 3D as shown in Figures S7 and 8. The intercubane distance (between nearest zinc atoms) was found to be 11.021(6) Å (Table S2), which is separated by a bipyridyl moiety (av 7.296 Å). Thus, individual D4R zinc phosphate cages in **4** act as tetrahedral four-connected nodes linked together by 4,4′-bipyridine spacers (Figure 3). This leads to the growth of a robust three-dimensional diamondoid framework featuring porous channels running along the *c* crystallographic axis (Figure 8). However, the apertures of these dumbbell-shaped channels measure only 2.9 × 0.5 nm^2 and do not allow efficient intrusion of guest molecules inside the channels. In compound **4**, the 2,6-diisopropyl groups from phosphate ligands are protruding into the channels and thus reduce the guest accessibility of this framework. The Langmuir surface area of this 3D framework solid measures only 255 m^2/g, which is marginal as compared to that observed for open framework nanoporous metal phosphates.[16] However, the ability to interconnect zinc phosphate D4R cages through robust coordinate linkages in a premeditated fashion is an important milestone in the development of designer zeolitic solids. Compound **4** represents a hitherto unknown example of a 3D zinc phosphate framework prepared from preformed molecular building block.

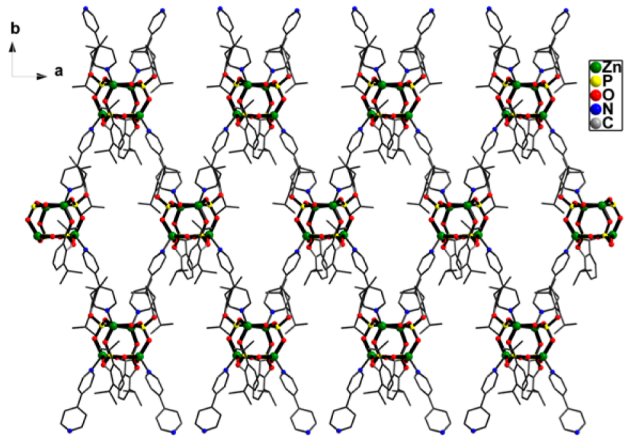

Figure 8. View of channels along the *c* axis of compound **4**.

Synthesis and Characterization of $[Zn_4(dipp)_4(L)_2]$ (L = L3 (5), L4 (6), L5 (7)). As the guest accessibility in compound **4** is squeezed due to the presence of bulky isopropyl groups, it was initially anticipated that employing monoorganophosphate esters possessing less bulky aryl substituents will enhance the porosity of the 3D frameworks. However, all manipulations involving 2,6-dimethylphenyldihydrogen phosphate were futile due to the difficulty in isolating crystalline products. Therefore, the only other possibility to enhance porosity is by placing the D4R cages far apart through employment of longer bipyridine spacers. In order to corroborate the feasibility of this route, the reaction leading to **4** was carried out by utilizing a longer spacer L3−L5 instead of L1. The reaction of $[Zn(dipp)(DMSO)]_4$ with bipyridine spacers L3−L5 resulted in the precipitation of **5**−**7** as microcrystalline powders in 92, 97, and 95% yield, respectively. The isolated product has been characterized by analytical and spectroscopic techniques.

In the FT-IR spectra, strong peaks appearing at 1173−1183, 1020−1021, and 915−919 cm^{-1} are due to the P═O stretching vibrations and M−O−P asymmetric and symmetric stretching vibrations, respectively (Figures S8, S9, and S10).[11] A peak at around 2299 cm^{-1} for **6** can be assigned to the acetylene group of the bipyridyl moiety (Figure S9). ^{1}H NMR spectra of **5**−**7** show well-separated peaks for all protons of dipp and bipyridine moieties (Figures S9). The ^{1}H NMR spectra of all three compounds feature two doublets appearing in the range δ 8.9 to 7.0 ppm, and these can be easily attributed to the aromatic protons of the dipyridyl group. The resonance around δ 7.6 ppm in **5** is due to the $-CH_2$ group of the ethylene bridge, which is missing in the case of **6**. In the case of **7**, the proton NMR spectrum shows two triplets at δ 2.5 and 1.9 ppm for the propyl bridge of bipyridine (L5). The multiplet observed in the range δ 7.0−6.9 ppm for **5**−**7** is due to the aromatic protons of the dipp moiety. A septet appears at around δ 3.6 ppm due to the −CH protons of the dipp isopropyl group. A doublet at δ 1.1 ppm is due to the $-CH_3$ protons of the dipp isopropyl moiety. Integration of the ^{1}H NMR spectra gives an idea of formation of supramolecular assemblies with a dipp:bipyridine ratio of 1:0.5. In the ^{31}P NMR spectra of **5**−**7** (Figures S10), a single resonance is

dx.doi.org/10.1021/ic500810d | Inorg. Chem. 2014, 53, 8959−8969

observed due to the nearly identical chemical environment for the dipp phosphorus atoms of these supramolecular assemblies.

To study the porosity of framework solid **5**, N_2 absorption measurements were performed at 77 K. For this purpose, the synthesized materials were evacuated to remove any guest solvent molecules by evacuation under a dynamic vacuum at 100 °C. The Langmuir surface area for compound **5** has been measured to be 279 m^2/g (Figure 9). A modest enhancement

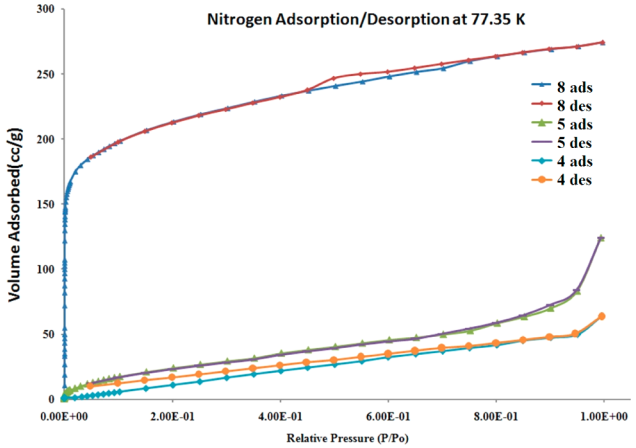

Figure 9. N_2 adsorption isotherms of **4**, **5**, and **8** at 77 K.

of surface area for **5** as compared to **4** can easily be attributed to the increase in spacer length. Although the enhancement of surface area is not noteworthy, the isolation of **5** establishes the feasibility to produce isoreticular zinc phosphate frameworks by employing different bipyridine spacers. Thus, the prospective guest-accessible porosity enhancement of zinc phosphate frameworks by proper choice of linkers cannot be ruled out at this stage. N_2 physisorption measurements for **6** and **7** result in a very low surface area, which is likely to be the result of manyfold interpenetration of the frameworks. To evaluate the potential of these frameworks as hydrogen storage media, hydrogen adsorption was performed at 77 K. Figure 10 shows hydrogen adsorption isotherms of **5**.

Synthesis and Characterization of $[Zn_4(dipp)_4(L6)_2]$ (8). Driven by the successful relative enhancement of porosity

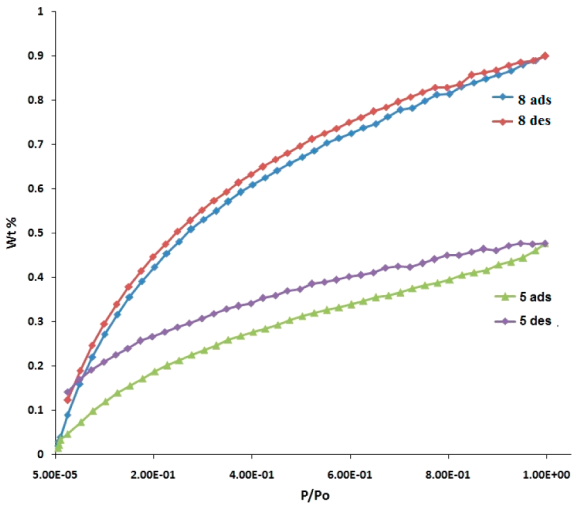

Figure 10. H_2 adsorption isotherms of **5** and **8** at 77 K.

by incorporation of a longer spacer, we endeavored to further lengthen the spacers in order to modulate the guest accessibility within zinc phosphate frameworks. The reaction of $[Zn(dipp)(DMSO)]_4$ with a tetrazine-based rigid linear spacer L6 leads to the formation of $[Zn_4(dipp)_4(L6)_2]$ (**8**). In the FT-IR spectrum of **8**, strong peaks appearing at 1173, 1020, and 918 cm^{-1} were due to the P═O stretching vibrations and M−O−P asymmetric and symmetric stretching vibrations, respectively (Figure S11).[11] Two doublets observed in the ^1H NMR spectrum at δ 8.9 and 8.4 ppm are due to the aromatic protons of dipyridyl ligand L6 (Figure S11). The multiplet appearing at δ 7.0 ppm is assigned to the aromatic protons of the dipp moiety. A septet resonance appears for **8** at around δ 3.6 ppm due to the −CH protons of the dipp isopropyl group. A doublet appearing at δ 1.1 ppm is due to the $-CH_3$ protons of the dipp isopropyl moiety. In the ^{31}P NMR spectrum of **8**, a singlet is observed at δ −5.2 ppm due to the presence of phosphorus atoms of the dipp ligand (Figure S11).

Compound **8** crystallizes in a tetragonal system with the *P*4/*nnc* space group. The basic structural unit of **8** is shown in Figure 11. As anticipated the longer spacer L6 assists to bridge the four-connected D4R nodes into a robust coordination framework featuring channels running along the crystallographic axis (Figure 11). Precise topological analysis of the framework using the TOPOS program revealed that the compound has a 4-fold interpenetrated diamondoid network with a 4c-uninodal structure with point symbol $\{3^3.12^3\}$ (Figure 11).[14] Due to extensive interpenetration of the diamondoid networks, the effective aperture of the hexagonal channels shrunk to almost half of the expected aperture and thus greatly reduced the capability of the framework to accommodate guest molecules. Although the diamondoid networks in **8** are interpenetrated, the Langmuir surface area of **8** measured 1147 m^2/g. Thus, compound **8** represents a fine example of a highly porous metal phosphate framework assembled by coordinatively interlinking D4R cages. Hydrogen uptake of **8** at 77 K and 760 Torr measures ∼1.0 wt % (Figure 10). PXRD measurements of the activated sample of **8** provides a pattern similar to that simulated from SCXRD data, revealing the integrity of the framework structure after evacuation (Figure S15).

Synthesis and Characterization of $[Zn_4(dipp)_4(L7)_2]$ (9). The ability to incorporate longer spacers without altering the framework connectivity establishes the susceptibility of the present methodology to any change in the linker molecule. It was therefore anticipated that the physical or chemical environment within the pores of the zinc phosphate frameworks can be easily modulated by proper choice of linkers. Regulating the physical/chemical environment of pores within framework solids has remained one of the most pressing requirements for their eventual application in industry. By employing the redox-active, naphthalene-based rigid and relatively longer spacer L7, $[Zn_4(dipp)_4(L7)_2]$ (**9**) can be isolated in good yield.

In the FT-IR spectrum of **9** strong peaks appearing at 1175, 1019, and 918 cm^{-1} are due to the P═O stretching vibrations and M−O−P asymmetric and symmetric stretching vibrations, respectively (Figure S12).[11] The absorption at around 1684 cm^{-1} for **9** can be assigned to the C═O group of L7. As expected, the ^1H NMR spectrum of **9** shows peaks for all the protons of dipp and bipyridine moieties in a dipp:bipyridine ratio of 1:0.5 (Figure S12). The three resonances observed at δ 8.7 (two peaks merged) and 7.6 ppm are due the aromatic

dx.doi.org/10.1021/ic500810d | Inorg. Chem. 2014, 53, 8959−8969

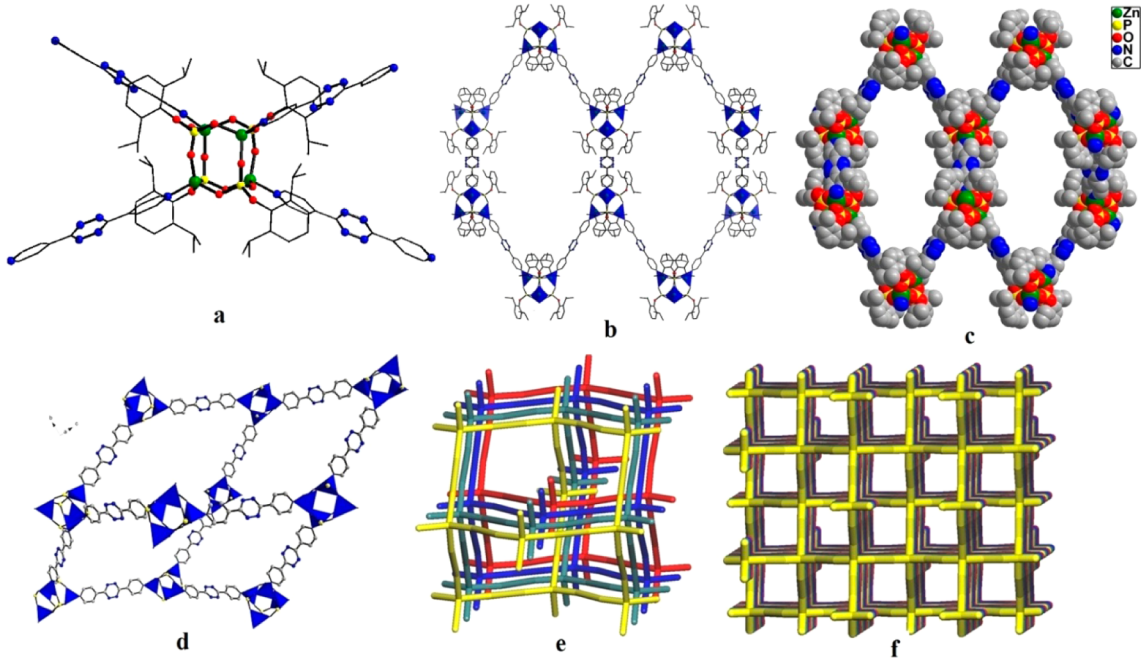

Figure 11. Perspective view of **8**: (a) ball-and-stick model of a single unit; (b) hexagonal channel in **8**; (c) space-filling model of the hexagonal channel; (d) diamondoid cage present in **8**; (e) stick model showing 4-fold interpenetration of the diamondoid cage in **8**; (f) stick model showing the interpenetrated network.

protons of the dipyridyl ligand. The multiplet appearing at δ 6.9 ppm in **9** is due to the aromatic protons of the dipp moiety. A septet resonance appearing at δ 3.6 ppm is due to the methine protons of the dipp isopropyl group. A doublet appearing at δ 1.1 ppm is assignable to the $-CH_3$ protons of the dipp isopropyl group. As before, the ^{31}P NMR spectrum of **9** also shows a single resonance at around δ −5.2 ppm (Figure S12).

Compound **9** crystallizes in the orthorhombic *Fddd* space group, and as expected, the linker L7 coordinatively interconnects the tetrahedral D4R nodes (Figure 12), leading

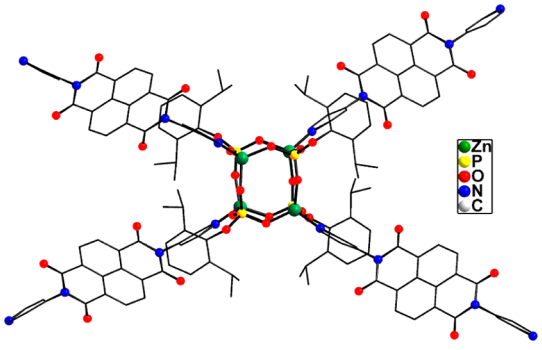

Figure 12. Ball-and-stick model of the D4R core bridged by L7 in **9**. Hydrogen atoms have been omitted for clarity.

to the formation of a robust 3D diamondoid framework. Topological analysis of the framework structure using the TOPOS program suggests that compound **9** is a 5-fold interpenetrated diamondoid network, and a stick-model representation of the interpenetrated framework structure is depicted in Figure 13. The 4c-uninodal structure can be represented by the point symbol $\{3^3.12^3\}$.[14] Due to extensive interpenetration of the diamondoid framework, the measured Langmuir surface area for **9** is only 128 m^2/g, which is marginal when compared to that observed for **8**. However, the adaptability of the zinc phosphate framework to linkers vastly different from the bipyridine-based linkers used earlier opens up fascinating frontiers to build functional zeolites. It is pertinent to note here that the present linker, L7, has been earlier employed to integrate redox-active Zn-carboxylate-based metal organic frameworks.[17] Such redox-active frameworks are anticipated to be highly relevant in doping specific ions into the framework structure through the interplay of electrostatic interactions.

THERMAL PROPERTIES

The thermal behavior of **1**−**9** has been investigated in the temperature range 25−800 °C under a stream of nitrogen gas (Figure S13). The most striking feature seen in the plot is the significant thermal stability of these framework compounds. Barring the loss of any solvent molecules such as methanol from the porous structure, the new framework structures are stable until 250−350 °C. For compounds **1**−**9**, a weight loss in the temperature range 250−500 °C, due to the organic part or aryl moiety, results in the exclusive formation of zinc pyrophosphate, $[Zn_2P_2O_7]$, which is consistent with the thermal decomposition product of zinc di-*tert*-butylphosphate complexes reported earlier.[18]

CONCLUSIONS

A first ever stepwise hierarchical and rational synthesis of porous solids by the predictable and directed assembly of easily isolable molecular building blocks has been achieved for any given system, be it silicates, phosphates, carboxylates, or any other type. The highly complex and unpredictable nature of the preparation of zeolitic porous solids has been overcome through utilization of a soluble D4R zinc phosphate cage as the building block. Moreover the preparative procedures are simple and do not require high pressure or temperature. Another remarkable feature of the present methodology is that the isolable, preformed, and highly robust D4R SBU can be

dx.doi.org/10.1021/ic500810d | *Inorg. Chem.* 2014, 53, 8959−8969

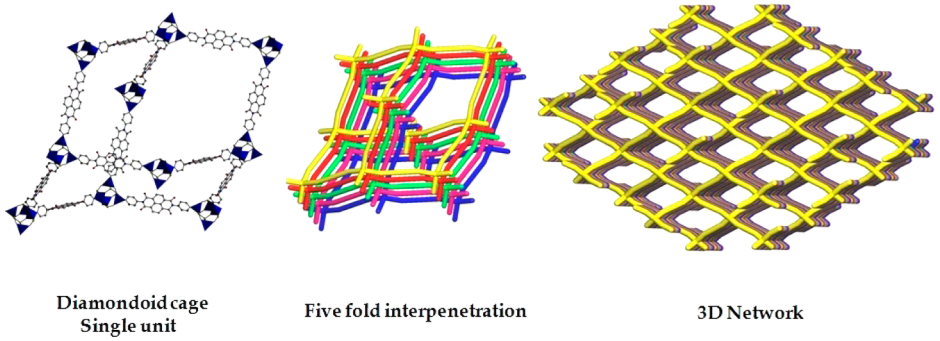

Figure 13. Fivefold interpenetrated diamondoid network and 3D framework structure in **9**.

interconnected through a varied choice of bipyridine-based spacers to isolate hierarchical superstructures. Surface area measurements of these framework solids show that the porous nature can be tuned by suitable modification of spacers. Moreover the ability to isolate robust crystalline frameworks by incorporating bipyridine spacers featuring different functionality opens up new prospectives for their utilizations in versatile applications far beyond their traditional use as catalysts, adsorbents, or ion exchange materials. Finally, the hierarchical room-temperature 3D porous structure building approach described in this contribution nicely complements the metal–organic frameworks (MOFs),[19] which have assembled from carboxylic acid derivatives, albeit prepared normally under hydrothermal conditions in one pot. The correlation between these two approaches can be exploited to build newer hybrid porous solids in the future. Currently these possibilities are being explored in our laboratory.

EXPERIMENTAL SECTION

Instruments and Methods. All reactions were carried out under a fume hood in beakers, test tubes, or round-bottom flasks with special precautions for crystallization, as most of the reaction immediately gives a copious amount of noncrystalline precipitate on simple mixing. All the starting materials and the products were found to be stable toward moisture and air, and no specific precaution was taken to rigorously exclude air. The melting points were measured in glass capillaries and are reported uncorrected. Infrared spectra were obtained on a PerkinElmer Spectrum One FT-IR spectrometer as KBr diluted discs. Microanalyses were performed on a Thermo Finnigan (FLASH EA 1112) microanalyzer. NMR spectra were recorded using a Varian 400 MHz and a Bruker Advance DPX-400 spectrometer. Thermogravimetric analysis was carried out on a PerkinElmer thermal analysis system under a stream of nitrogen gas at a heating rate of 10 °C/min. Commercial grade solvents were purified by employing conventional procedures, and other chemicals such as 4,4′-dipyridyl (Sigma-Aldrich), 1,2-di(pyridin-4-yl)ethene (Sigma-Aldrich), $Zn(OAc)_2{\cdot}2H_2O$ (S.d.Fine-Chem.) were used as received. 2,6-Di-isopropylphenyl dihydrogen phosphate, L2, L4, L6, and L7 were synthesized according to the published procedure.[20−22]

1: A solution of $dippH_2$ (0.258 g, 1 mmol) and $Zn(OAc)_2{\cdot}2H_2O$ (0.219 g, 1 mmol) in 30 mL of methanol was stirred for 10 min. The resultant mixture was stirred to obtain a clear solution, and then DMSO (2 mL) was added. The reaction mixture was filtered, and the filtrate was kept on the benchtop for crystallization at 25 °C. Block-shaped single crystals of **1** were obtained from the reaction mixture after 3−4 days. Yield: 0.38 g (97% based on $dippH_2$), Mp: >275 °C. Anal. Calcd for $[C_{56}H_{92}Zn_4P_4O_{20}S_4]$ (M_r = 1599): C, 42.06; H, 5.80; S, 8.02. Found: C, 42.99; H, 6.08; S, 8.12. IR (KBr, cm^{-1}): 3449(br), 2962(s), 2928(w), 2867(w), 1650(br), 1468(s), 1443(w), 1382(w), 1361(w), 1340(s), 1257(s), 1175(vs), 1046(w), 1019(vs), 955(s), 918(vs), 882(w), 805(w), 772(s), 551(s). ^{1}H NMR (DMSO-d_6, 300 MHz): δ 6.93−7.06 (m, 3H, Ar), 3.88 (septet, 2H, ^{i}Pr-CH, $^3J_{HH}$ = 6.9 Hz), 2.52 (s, 12H, CH_3), 1.16 (d, 12H, ^{i}Pr-CH_3). ^{31}P NMR (DMSO-d_6, 121 MHz): δ −4.9 ppm.

2: A solution of $dippH_2$ (0.258 g, 1 mmol) in methanol (20 mL) was added to a methanolic solution (10 mL) of $Zn(OAc)_2{\cdot}2H_2O$ (0.219 g, 1 mmol). The solution was stirred to obtain a clear solution and diluted by a methanol−DMSO mixture (140:30 mL). To that was added dropwise L1 (0.078 g, 0.5 mmol) in methanol (20 mL) over the period of 2 h at room temperature. The resulting clear solution was left undisturbed at room temperature on the benchtop for crystallization. Colorless single crystals of **2** were obtained after 24 h. Yield: 0.35 g (85%). Mp: >275 °C. Anal. Calcd for $[C_{134}H_{184}N_6O_{36}P_8S_4Zn_8]$ (M_r = 3354.2): C, 47.98; H, 5.53; N, 2.51; S, 3.82. Found: C, 46.46; H, 5.25; N, 3.03; S, 2.06. IR (KBr, cm^{-1}): 3433(br), 3068(w), 2963(s), 2927(w), 2868(w), 1612(s), 1536(w), 1467(s), 1443(s), 1420(w), 1382(w), 1339(s), 1257(s), 1175(vs), 1046(w), 1020(vs), 914(s), 881(w), 815(w), 771(s).

3: To a solution of $Zn(OAc)_2{\cdot}2H_2O$ (0.219 g, 1 mmol) in 50 mL of methanol was added $dippH_2$ (0.258 g, 1 mmol), and the mixture was stirred for 10 min to obtain a clear solution. The resultant mixture was filtered into a flask and diluted to 170 mL, and to this was added dropwise L2 (0.09 g, 0.5 mmol) in 5 mL of methanol. The solution was kept undisturbed for a few days. Single crystals of **3** were obtained from the reaction mixture after 4 days. Yield: 0.31 g (80%). Mp: >275 °C. Anal. Calcd for $[C_{66}H_{92}N_6O_{19}P_4Zn_4]$ (M_r = 1559.0): C, 47.78; H, 5.59; N, 5.07. Found: C, 47.09; H, 5.33; N, 5.01. FT-IR (KBr, cm^{-1}): 3429(br), 2965(s), 2869(s), 1606 (s), 1442(s), 1256(s), 1172(vs), 1030(vs), 915(vs), 772(vs), 745(s). ^{1}H NMR (DMSO-d_6, 400 MHz): δ 8.8, 8.28, 7.82, 7.0 (m), 3.6 (septet), 3.5, 1.06 (d) ppm. ^{31}P NMR (DMSO-d_6, 400 MHz): δ −4.60 ppm.

4: To a solution of L1 (0.0097g, 0.0621 mmol) in about 100 mL of methanol was added a methanolic (10 mL) solution of $[Zn(dipp)(DMSO)]_4$ (0.025 g, 0.0156 mmol), and the mixture was kept undisturbed for crystallization on the benchtop. Crystals of **4** were obtained from the reaction mixture after 1 day. Yield: 0.023 g (95%). Mp: >275 °C. Anal. Calcd for $[C_{68}H_{84}N_4O_{16}P_4Zn_4]$ (M_r = 1598.94): C, 51.08; H, 5.30; N, 3.50. Found: C, 49.68; H, 5.47; N, 3.46. FT-IR (KBr, cm^{-1}): 3462(br), 2960(vs), 2866(vs), 1612(vs), 1466(vs), 1440(s), 1175(vs), 1070(vs), 1020(vs), 916(vs), 768(vs), 641(s). ^{1}H NMR (DMSO-d_6, 400 MHz): δ 8.7 (d 2H, $^3J_{HH}$ = 5.93 Hz, *ortho*-N), 7.8 (d, 2H, $^3J_{HH}$ = 6.1 Hz, *meta*-N), 6.9 (m, 6H, $^3J_{HH}$ = 6.9 Hz, Ar), 3.6 (septet, 4H, $^3J_{HH}$ = 6.7 Hz, ^{i}Pr-CH), 1.08 (d, 24H, $^3J_{HH}$ = 6.8 Hz, ^{i}Pr-CH_3) ppm. ^{31}P NMR (DMSO-d_6, 400 MHz): δ −5.2 ppm.

5: To a solution of L3 (0.018 g, 0.1 mmol) in about 100 mL of methanol was added a methanol (10 mL) solution of $[Zn(dipp)(DMSO)]_4$ (0.0399 g, 0.025 mmol), and the mixture was kept undisturbed for crystallization on the benchtop. Precipitates of **5** were obtained after 2−3 h as a white solid. Yield: 0.04 g (92%). Mp: >275 °C. Anal. Calcd for $[C_{72}H_{88}N_4O_{16}P_4Zn_4]$ (M_r = 1651.02): C, 52.38; H, 5.37; N, 3.39. Found: C, 53.23; H, 5.32; N, 3.15. FT-IR (KBr, cm^{-1}): 3435(br), 2963(vs), 2867(s), 1614(vs), 1435(s), 1337(s), 1256(s), 1176(vs), 1069(w), 1020(vs), 915(vs), 771(vs), 553(vs). ^{1}H NMR (DMSO-d_6, 400 MHz): δ 8.5 (d, 2H, $^3J_{HH}$ = 5.93 Hz, *ortho*-N), 7.6 (d, 2H, $^3J_{HH}$ = 4.64 Hz, *meta*-N), 7.6 (s, 1H), 7.0 (m, 3H, $^3J_{HH}$ = 6.9 Hz,

dx.doi.org/10.1021/ic500810d | Inorg. Chem. 2014, 53, 8959−8969

Table 1. Crystal Data and Structure Refinements Details for 1−4, 8, and 9

	1	2	3	4	8	9
formula	$C_{56}H_{92}O_{20}P_4S_4Zn_4$	$C_{134}H_{184}N_6O_{36}P_8S_4Zn_8$	$C_{66}H_{92}N_6O_{19}P_4Zn_4$	$C_{68}H_{84}N_4O_{16}P_4Zn_4$	$C_{76}H_{90}N_{12}O_{20}P_4Zn_4$	$C_{96}H_{92}N_8O_{24}P_4Zn_4$
fw	1598.90	3353.83	1658.82	1598.75	1877.03	2127.24
temp [K]	566(2)	293(2)	150(2)	123(2)	93(2)	113(2)
cryst syst	triclinic	monoclinic	monoclinic	orthorhombic	tetragonal	orthorhombic
space group	$P\bar{1}$	*Pc*	$P2_1/c$	*Fdd*2	*P*4/*nnc*	*Fddd*
a [Å]	14.282(4)	18.846(3)	14.862(3)	27.663(4)	17.980(2)	10.358(3)
b [Å]	16.100(4)	25.339(4)	25.015(4)	49.610(2)	17.980(2)	44.783(1)
c [Å]	17.397(4)	17.390(3)	22.180(6)	27.879(1)	30.999(3)	70.000(2)
α [deg]	76.491(2)	90	90	90	90	90
β [deg]	67.172(2)	102.082(2)	109.026(2)	90	90	90
γ [deg]	87.533(2)	90	90	90	90	90
V [Å^3]	3580.06(2)	8121(2)	7795.4(3)	38260(2)	10021(2)	32468(15)
Z	2	2	4	16	4	8
D(calcd) [g/cm^3]	1.483	1.372	1.413	1.111	1.166	0.870
μ [mm^{-1}]	1.595	1.360	1.367	1.109	1.066	0.6698
cryst size [mm^3]	0.3 × 0.2 × 0.15	0.4 × 0.3 × 0.03	0.40 × 0.36 × 0.33	0.23 × 0.12 × 0.11	0.14 × 0.04 × 0.04	0.35 × 0.10 × 0.05
θ range [deg]	3.30 to 28.28	1.61 to 23.61	3.33 to 32.86	3.66 to 25.21	3.08 to 27.48	2.00 to 22.50
no. of rflns collected	36 520	23 884	88 434	116 328	36 989	33 885
indep reflns ($I_0 > 2\sigma(I_0)$)	17 726	12 572	26 509	17 159	5751	5207
GOF	0.886	1.085	0.912	0.765	1.113	1.077
R1 ($I_0 > 2\sigma(I_0)$)	0.0440	0.0709	0.0472	0.0494	0.0674	0.0984
wR2 (all data)	0.1107	0.1877	0.0997	0.1067	0.2164	0.3205
largest hole and peak [e·Å^{-3}]	−1.414, 1.637	−0.769, 2.167	−0.629, 0.975	−0.394, 0.756	−0.867, 1.084	−0.52, 0.61

dx.doi.org/10.1021/ic500810d | *Inorg. Chem.* 2014, 53, 8959−8969

Ar), 3.6 (septet, 2H, $^3J_{HH}$ = 6.7 Hz, ^{i}Pr-CH), 1.07 (d, 12H, $^3J_{HH}$ = 6.8 Hz, ^{i}Pr-CH_3) ppm. ^{31}P NMR (DMSO-d_6, 161 MHz): δ −5.2 ppm.

6: To a solution of 1,2-di(4-pyridyl)ethyne (L4) (0.018 g, 0.1 mmol) in about 100 mL of methanol was added $[Zn(DMSO)(dipp)]_4$ (0.0399 g, 0.025 mmol) in 10 mL of methanol. The product was isolated as a white solid immediately after mixing. Yield: 0.04 g (97%). Mp: >275 °C. Anal. Calcd for $[C_{72}H_{84}N_4O_{16}P_4Zn_4]$ (M_r = 1646.99): C, 52.51; H, 5.14; N, 3.40. Found: C, 51.51; H, 4.99; N, 2.58. FT-IR (KBr, cm^{-1}): 3430(br), 2964(vs), 2867(s), 2299(s), 1614(vs), 1440(s), 1361(s), 1256(s), 1175 (vs), 1046(w), 1020(vs), 919(vs), 772(vs), 549(vs). ^{1}H NMR (DMSO-d_6, 400 MHz): δ 8.6 (d 2H, $^3J_{HH}$ = 5.26 Hz, *ortho*-N), 7.6 (d, 2H, $^3J_{HH}$ = 5.92 Hz, *meta*-N), 6.9 (m, 3H, $^3J_{HH}$ = 5.9 Hz, Ar), 3.6 (septet, 2H, $^3J_{HH}$ = 6.8 Hz, ^{i}Pr-CH), 1.0 (d, 12H, $^3J_{HH}$ = 6.8 Hz, ^{i}Pr-CH_3) ppm. ^{31}P NMR (DMSO-d_6, 161 MHz): δ −5.2 ppm.

7: To a solution of 1,2-di(4-pyridyl)propane (L5) (0.019 g, 0.1 mmol) in about 100 mL of methanol was added $[Zn(dipp)(DMSO)]_4$ (0.0399 g, 0.025 mmol) in 10 mL of methanol, and the mixture was kept undisturbed for crystallization on the benchtop. After an hour, a precipitate starts to appear as a white solid. Yield: 0.04 g (95%). Mp: >275 °C. Anal. Calcd for $[C_{74}H_{96}N_4O_{16}P_4Zn_4]$ (M_r = 1683.11): C, 52.81; H, 5.75; N, 3.33. Found: C, 53.06; H, 5.01; N, 3.45. FT-IR (KBr, cm^{-1}): 3445(br), 2960(s), 2867(s), 1620(vs), 1434(s), 1337(s), 1256(s), 1183(vs), 1069(w), 1021(vs), 913(vs), 772(vs), 558(s), 527(s). ^{1}H NMR (DMSO-d_6, 400 MHz): δ 8.4 (d 2H, $^3J_{HH}$ = 5.93 Hz, *ortho*-N), 7.2 (d, 2H, $^3J_{HH}$ = 4.76 Hz, *meta*-N), 7.0 (m, 3H, $^3J_{HH}$ = 5.4 Hz, Ar), 3.6 (septet, 2H, $^3J_{HH}$ = 6.5 Hz, ^{i}Pr-CH), 2.5 (t, 4H, $^3J_{HH}$ = 7.6, Py-CH_2), 1.9, (t, 2H, $^3J_{HH}$ = 7.69, Py-CH$_2$-CH_2) 1.0 (d, 12H, $^3J_{HH}$ = 6.5 Hz, ^{i}Pr-CH_3) ppm. ^{31}P NMR (DMSO-d_6, 161 MHz): δ −5.2 ppm.

8: To a solution of L6 (0.024 g, 0.1 mmol) in 100 mL of methanol was added $[Zn(dipp)(DMSO)]_4$ (0.0399 g, 0.025 mmol) in 10 mL of methanol, and the mixture was kept undisturbed for crystallization on the benchtop. Crystals of **6** were obtained from the reaction mixture after 2 days. Yield: 0.04 g (90%). Mp: >275 °C. Anal. Calcd for $[C_{76}H_{90}N_{12}O_{20}P_4Zn_4]$ (M_r = 1877.13): C, 48.63; H, 4.83; N, 8.95. Found: C, 44.42; H, 4.53; N, 9.34. FT-IR (KBr, cm^{-1}): 3447(br), 2964(vs), 2869(s), 1620(vs), 1437(s), 1393(s), 1256(s), 1173(vs), 1060(s), 1020(vs), 918(vs), 774(vs), 602(vs). ^{1}H NMR (DMSO-d_6, 400 MHz): δ 8.9 (d 2H, $^3J_{HH}$ = 4.5 Hz, *ortho*-N), 8.4 (d, 2H, $^3J_{HH}$ = 4.4 Hz, *meta*-N), 7.0 (m, 3H, $^3J_{HH}$ = 6.7 Hz, Ar), 3.6 (sept, 2H, $^3J_{HH}$ = 6.9 Hz, ^{i}Pr-CH), 1.09 (d, 12H, $^3J_{HH}$ = 6.8 Hz, ^{i}Pr-CH_3) ppm. ^{31}P NMR (DMSO-d_6, 161 MHz): δ −5.2 ppm.

9: To a solution of L7 (0.0260 g, 0.0621 mmol) in about 100 mL of methanol was added a methanolic (10 mL) solution of $[Zn(dipp)(DMSO)]_4$ (0.025 g, 0.0156 mmol) slowly over an interval of half an hour, and the mixture was kept undisturbed for crystallization on the benchtop. Crystals of **7** were obtained from the reaction mixture after 3 days. Yield: 0.02 g (70%). Mp: >275 °C. Anal. Calcd for $[C_{24}H_{23}N_2O_6PZn]$ (M_r = 531.78): C, 54.20; H, 4.36; N, 5.27. Found: C, 51.99; H, 3.82; N, 4.75. FT-IR (KBr, cm^{-1}): 3422(br), 2963(vs), 2926(s), 2867(vs), 1723(vs), 1684(vs), 1612(vs), 1581(vs), 1444(vs), 1344(vs), 1248(vs), 1175(vs), 1099(s), 1019(vs), 918(vs), 766(vs), 532(vs). ^{1}H NMR (DMSO-d_6, 400 MHz): δ 8.77(d, 2H, $^3J_{HH}$ = 4.60 Hz, *ortho*-N), 7.60 (d, 2H, $^3J_{HH}$ = 5.64 Hz, *meta*-N), 6.9 (m, 6H, $^3J_{HH}$ = 6.24 Hz, Ar), 3.67 (septet, 4H, $^3J_{HH}$ = 6.84 Hz, ^{i}Pr-CH), 1.08 (d, 24H, $^3J_{HH}$ = 6.84 Hz, ^{i}Pr-CH_3) ppm. ^{31}P NMR (DMSO-d_6, 400 MHz): δ −5.2 ppm.

Single-Crystal X-ray Diffraction Studies. The X-ray diffraction intensities for **1**−**4** were collected on an Oxford Xcalibur 2 diffractometer equipped with a Sapphire2 CCD. The determinations of unit cell parameters and data collections were performed with "Mo Kα" radiation (λ = 0.7107 Å). Diffraction intensities for **8** and **9** were collected on a Rigaku Saturn 724+ CCD diffractometer. Data integration and indexing using CrysAlisPro[23] (for **1**−**4**) and CrystalClear-SM Expert (for **8** and **9**) were followed by calculations using the programs in the WinGX module[24] and solved by direct methods (SIR-92).[25] The final refinement of the structure was carried out using full least-squares methods on F^2 using SHELXL-97,[26] resulting in the structure determination for all the compounds. The final refinement of **1**−**4**, **8**, and **9** converged at R values of 0.0440, 0.0709, 0.0472, 0.0494, 0.0674, and 0.0984 ($I > 2\sigma(I)$) respectively. In all cases all non-hydrogen atoms were refined anisotropically. Crystal data and structure refinement details for all compounds are listed in Table 1; details regarding disordered group treatment and the extent of solvent-accessible voids in each of the crystal structure are described in the Supporting Information.

Gas Adsorption Measurements. Gas adsorption measurements were performed using a Quantachrome Autosorb-1C analyzer. UHP-grade gases were used in measurements without further purification. The N_2 measurements were done at 77 K in a liquid nitrogen bath. Since all frameworks contain solvent molecules inside the pores, a solvent exchange method has been employed to activate the pores. Crystals of each compound were washed with dry methanol several times and kept in a sample vial for 2−3 days in methanol. During this period solvent was refilled in a 4−5 h interval of time. After that, crystals were transferred to a round-bottom flask (without letting the crystals dry) and evacuated for about 10 to 12 h. Then the round-bottom flask was heated slowly to 100 °C by using a silicon oil bath, and the crystals were evacuated for 24−28 h. The activated sample was cooled to room temperature under nitrogen and submitted for adsorption analysis. Again before gas adsorption measurements, the sample was evacuated at room temperature (for 4 h) and 100 °C (for 5 h) under ultrahigh vacuum (10^{-8} mbar) built in the Autosorb-1C after transferring the compounds to the sample holder.

■ ASSOCIATED CONTENT

Ⓢ Supporting Information

Detailed experimental procedures, X-ray crystallographic information (Table 1), and analytical and spectroscopic data are provided. CCDC-923202−923207 (**1**−**4**, **8**, and **9**). This material is available free of charge via the Internet at http://pubs.acs.org.

■ AUTHOR INFORMATION

Corresponding Author

*E-mail: rmv@chem.iitb.ac.in. Fax: +91 22 25767152. Phone: +91 22 2576 7163.

Notes

The authors declare no competing financial interest.

■ ACKNOWLEDGMENTS

This work was supported by Nanomission, DST, New Delhi (Project: SR/NM/NS-1119/2011) and DAE-BRNS, Mumbai (Project: 2010/21/04-BRNS). R.M. thanks BRNS for a DAE-SRC Outstanding Investigator Award. N.G. and R.J. thank CSIR, New Delhi, for research fellowships.

■ REFERENCES

(1) Wilson, S. T.; Lok, B. M.; Messina, C. A.; Cannan, T. R.; Flanigen, E. M. *J. Am. Chem. Soc.* **1982**, *104*, 1146−1147.

(2) (a) Rao, C. N. R.; Natarajan, S.; Choudhury, A.; Neeraj, S.; Ayi, A. A. *Acc. Chem. Res.* **2001**, *34*, 80−87. (b) Neeraj, S.; Natarajan, S.; Rao, C. N. R. *Angew. Chem., Int. Ed.* **1999**, *38*, 3480−3483. (c) Rao, C. N. R.; Natarajan, S.; Neeraj, S. *J. Am. Chem. Soc.* **2000**, *122*, 2810−2817. (d) Rao, C. N. R.; Natarajan, S.; Neeraj, S. *J. Solid State Chem.* **2000**, *152*, 302−321. (e) Natarajan, S.; Neeraj, S.; Rao, C. N. R. *Solid State Sci.* **2000**, *2*, 87−98. (f) Loiseau, T.; Ferey, G. *J. Fluorine Chem.* **2007**, *128*, 413−422. (g) Lillerud, K. P.; Olsbye, U.; Tilset, M. *Top. Catal.* **2010**, *53*, 859−868. (h) Du, Y.; Yu, J.-H.; Li, J.-Y.; Pan, Q.-H.; Xu, R.-R. *Chin. J. Inorg. Chem.* **2006**, *22*, 1503−1506. (i) Nagarathinam, M.; Saravanan, K.; Phua, E. J. H.; Reddy, M. V.; Chowdari, B. V. R.; Vittal, J. J. *Angew. Chem., Int. Ed.* **2012**, *51*, 5866−5877.

(3) (a) Cheetham, A. K.; Férey, G.; Loiseau, T. *Angew. Chem., Int. Ed.* **1999**, *38*, 3268−3292. (b) Chen, J.; Li, L.; Yang, G.; Xu, R. *J. Chem. Soc., Chem. Commun.* **1989**, 1217−1218. (c) Maeda, K.; Kiyozumi, Y.; Mizukami, F. *Angew. Chem., Int. Ed. Engl.* **1994**, *33*, 2335−2337.

(d) Maeda, K.; Akimoto, J.; Kiyozumi, Y.; Mizukami, F. *Angew. Chem., Int. Ed. Engl.* **1995**, *34*, 1199−1201. (e) Dhingra, S. S.; Haushalter, R. C. *J. Chem. Soc., Chem. Commun.* **1993**, 1665−1667. (f) Chippindale, A. M.; Brech, S. J.; Cowley, A. R.; Simpson, W. M. *Chem. Mater.* **1996**, *8*, 2259−2264. (g) Xu, Y.; Koh, L. L.; An, L.; Xu, R.; Qiu, S. *J. Solid State Chem.* **1995**, *117*, 373−378. (h) Koh, L. L.; Xu, Y.; Du, H. B.; Pang, W. Q. *Stud. Surf. Sci. Catal.* **1997**, *105*, 373−380. (i) Sevov, S. C. *Angew. Chem., Int. Ed. Engl.* **1996**, *35*, 2630−2632. (j) Gier, T. E.; Harrison, W. T. A. *Angew. Chem., Int. Ed. Engl.* **1991**, *30*, 1169−1171. (k) Nenoff, T. M.; Harrison, W. T. A.; Gier, T. E.; Stucky, G. D. *J. Am. Chem. Soc.* **1991**, *113*, 378−379. (l) Harrison, W. T. A.; Gier, T. E.; Moran, K. L.; Nicol, J. M.; Eckert, H.; Stucky, G. D. *Chem. Mater.* **1991**, *3*, 27−29. (m) Parise, J. B.; Corbin, D. R.; Abrams, L.; Northrup, P.; Rakovan, J.; Nenoff, T. M.; Stucky, G. D. *Zeolites* **1994**, *14*, 25−34. (n) Harrison, W. T. A.; Gier, T. E.; Nicol, J. M.; Stucky, G. D. *J. Solid State Chem.* **1995**, *114*, 249−257. (o) Harrison, W. T. A.; Martin, T. E.; Gier, T. E.; Stucky, G. D. *J. Mater. Chem.* **1992**, *2*, 175−181. (p) Bonavia, G.; Haushalter, R. C.; Zubieta, J. *J. Solid State Chem.* **1996**, *126*, 292−299.

(4) Férey, G. *Chem. Mater.* **2001**, *13*, 3084−3098 and references therein.

(5) Harrison, W. T. A. *Curr. Opin. Solid State Mater. Sci.* **2002**, *6*, 407−413 and references therein.

(6) Murugavel, R.; Walawalkar, M. G.; Pothiraja, R.; Rao, C. N. R.; Choudhury, A. *Chem. Rev.* **2008**, *108*, 3549−3655 and references therein.

(7) Murugavel, R.; Voigt, A.; Walawalkar, M. G.; Roesky, H. W. *Chem. Rev.* **1996**, *96*, 2205−2236.

(8) Montero, M.; Voigt, A.; Teichert, M.; Uson, I.; Roesky, H. W. *Angew. Chem., Int. Ed.* **1995**, *34*, 2504−2506.

(9) Chandrasekhar, V.; Boomishankar, R.; Nagendran, S. *Chem. Rev.* **2004**, *104*, 5847−5910.

(10) (a) Walawalkar, M. G.; Roesky, H. W.; Murugavel, R. *Acc. Chem. Res.* **1999**, *32*, 117−126. (b) Murugavel, R.; Shanmugan, S. *Chem. Commun.* **2007**, 1257−1259. (c) Murugavel, R.; Shanmugan, S. *Dalton Trans.* **2008**, 5358−5367. (d) Murugavel, R.; Walawalkar, M. G.; Dan, M.; Roesky, H. W.; Rao, C. N. R. *Acc. Chem. Res.* **2004**, *37*, 763−774. (e) Murugavel, R.; Gogoi, N.; Clerac, R. *Inorg. Chem.* **2009**, *48*, 646−651.

(11) (a) Murugavel, R.; Kuppuswamy, S.; Boomishankar, R.; Steiner, A. *Angew. Chem., Int. Ed.* **2006**, *45*, 5536−5540. (b) Murugavel, R.; Kuppuswamy, S.; Gogoi, N.; Boomishankar, R.; Steiner, A. *Chem.—Eur. J.* **2010**, *16*, 994−1009. (c) Murugavel, R.; Kuppuswamy, S.; Gogoi, N.; Steiner, A. *Inorg. Chem.* **2010**, *49*, 2153−2162. (d) Murugavel, R.; Kuppuswamy, S. *Angew. Chem., Int. Ed.* **2006**, *45*, 7022−7026. (e) Murugavel, R.; Kuppuswamy, S.; Gogoi, N.; Boomishankar, R.; Steiner, A. *Chem.—Eur. J.* **2008**, *14*, 3869−3873. (f) Kalita, A. Ch.; Roch-Marchal, C.; Murugavel, R. *Dalton Trans.* **2013**, *42*, 9755. (g) Murugavel, R.; Kuppuswamy, S. *Inorg. Chem.* **2008**, *47*, 7686−7694. (h) Murugavel, R.; Kuppuswamy, S.; Randoll, S. *Inorg. Chem.* **2008**, *47*, 6028−6039. (i) Murugavel, R.; Kuppuswamy, S.; Maity, A. N.; Singh, M. P. *Inorg. Chem.* **2009**, *48*, 183−192. (j) Kalita, A. Ch.; Murugavel, R. *Inorg. Chem.* **2014**, *53*, 3345−3353.

(12) Walawalkar, M. G.; Murugavel, R.; Roesky, H. W.; Schmidt, H. G. *Organometallics* **1997**, *16*, 516−518.

(13) (a) Anantharaman, G.; Chandrasekhar, V.; Walawalkar, M. G.; Roesky, H. W.; Vidovic, D.; Magull, J.; Noltemeyer, M. *Dalton Trans.* **2004**, 1271−1275. (b) Chandrasekhar, V.; Kingsley, S.; Rhatigan, B.; Lam, M. K.; Rheingold, A. L. *Inorg. Chem.* **2002**, *41*, 1030−1032. (c) Chandrasekhar, V.; Sasikumar, P.; Boomishankar, R.; Anantharaman, G. *Inorg. Chem.* **2006**, *45*, 3344−3351. (d) Lugmair, C. G.; Tilley, T. D.; Rheingold, A. L. *Chem. Mater.* **1997**, *9*, 339−348. (e) Lugmair, C. G.; Tilley, T. D. *Inorg. Chem.* **1998**, *37*, 1821−1826. (f) Abufarag, A.; Vahrenkamp, H. *Inorg. Chem.* **1995**, *34*, 2207−2216. (g) Weis, K.; Rombach, M.; Vahrenkamp, H. *Inorg. Chem.* **1998**, *37*, 2470−2480. (h) Mao, J. G.; Clearfield, A. *Inorg. Chem.* **2002**, *41*, 2319−2324. (i) Fry, F. H.; Jensen, P.; Kepert, C. M.; Spiccia, L. *Inorg. Chem.* **2003**, *42*, 5637−5644. (j) Rivas, J. C. M.; Rosales, R. T. M.; Parsons, S. *J. Chem. Soc., Dalton Trans.* **2003**, 4385−4386.

(14) Blatov, V. A. *IUCrCompCommNewslett.* **2006**, *7*, 4−38.

(15) Pothiraja, R.; Shanmugan, S.; Walawalkar, M. G.; Butcher, R. J.; Nethaji, M.; Murugavel, R. *Eur. J. Inorg. Chem.* **2008**, 1834−1845.

(16) Guillou, N.; Gao, Q.; Forster, P. M.; Chang, J.-S.; Nogués, M.; Park, S.-E.; Férey, G.; Cheetham, A. K. *Angew. Chem., Int. Ed.* **2001**, *40*, 2831−2834.

(17) Ma, B.-Q.; Mulfort, K. L.; Hupp, J. T. *Inorg. Chem.* **2005**, *44*, 4912−4914.

(18) Murugavel, R.; Sathiyendiran, M.; Walawalkar, M. G. *Inorg. Chem.* **2001**, *40*, 427−434.

(19) (a) Zhou, H.-C.; Long, J. R.; Yaghi, O. M. *Chem. Rev.* **2012**, *112*, 673−674. (b) O'Keeffe, M.; Yaghi, O. M. *Chem. Rev.* **2012**, *112*, 675−702 and references therein.

(20) Kosolapoff, G. M.; Arpke, C. K.; Lamb, R. W.; Reich, H. J. *J. Chem. Soc.* **1968**, *7*, 815−818.

(21) Launay, J.-P.; Tourrel-Pagis, M.; Lipskier, J.-F.; Marvaud, V.; Joachim, C. *Inorg. Chem.* **1991**, *30*, 1033−1038.

(22) Farha, O. K.; Malliakas, C. D.; Kanatzidis, M. G.; Hupp, J. T. *J. Am. Chem. Soc.* **2010**, *132*, 950−952.

(23) *CrysAlisPRO*; Oxford Diffraction, Agilent Technologies UK Ltd: Yarnton, England.

(24) Farrugia, L. J. *WinGX*, Version 1.64.05. *J. Appl. Crystallogr.* **1999**, *32*, 837−838.

(25) Altomare, A.; Cascarano, G.; Giacovazzo, C.; Gualardi, A. *J. Appl. Crystallogr.* **1993**, *26*, 343−350.

(26) Sheldrick, G. M. *SHELXL-97*. *Acta Crystallogr. Sect. A* **2008**, *64*, 112−122.